

TRACING LUMINOUS AND DARK MATTER WITH THE SLOAN DIGITAL SKY SURVEY

J. LOVEDAY¹, for the SDSS collaboration

¹*Astronomy Centre, University of Sussex, Falmer, Brighton, BN1 9QJ, England*

Abstract. I summarize the scientific goals and current status of the Sloan Digital Sky Survey, briefly describe the Early Data Release, and discuss some recent scientific results obtained from commissioning data which are apposite to the distribution of luminous and dark matter in the Universe.

1 Introduction

The Sloan Digital Sky Survey (SDSS) is the most ambitious effort to date to map out the distribution of matter in the local Universe. A technical summary of the survey is given by York et al. [14]. Very briefly, the survey hardware comprises the 2.5-metre survey telescope, a 0.5-metre photometric telescope (called the monitor telescope in its previous incarnation), a state-of-the-art imaging camera [7] that observes near-simultaneously in five passbands $u'g'r'i'z'$ [5] and a pair of dual beam spectrographs, each capable of observing 320 fibre fed spectra. The data are reduced by a series of automated pipelines and the resulting data products stored in an object-oriented database.

The basic goal of the survey is to make a definitive map of the local Universe, consisting of 5-colour imaging over π sr to a depth $g' \approx 23$ and spectra of roughly one million galaxies and 100,000 QSOs. In this contribution, I will discuss the current survey status, the first public data release, and some science results obtained from commissioning data.

2 Survey Status

First light with the imaging camera was obtained on 9 May 1998 and the first extra-galactic spectra were obtained in June 1999. The survey was officially dedicated on 5 October 2000. At the time of writing (July 2001), we have imaged 3135 square degrees (24% of the total survey area) and obtained spectra for 366 plug-plates, yielding spectra for 158,000 galaxies, 20,000 QSOs and 27,000 stars, including some repeated observations. The spectrographs are performing extremely efficiently, with an overall throughput of 20% in the blue (3900–6000 Å) and 25% in the red (6000–9100 Å). Automated spectral reduction pipelines classify these spectra and measure redshifts. In roughly 8% of cases, the automated redshift measurement is in doubt and the spectrum is flagged for human inspection. About 1/8 of these (1% overall) had their redshift manually corrected. Based on manual inspection of all $\approx 23,000$ spectra from 39 plugplates, this procedure correctly measures redshifts for 99.7% of galaxies, 98.0% of quasars and 99.6% of stars.

3 The Early Data Release

The first public release of SDSS data (hereafter EDR) took place on 5 June 2001, and consists of images covering 460 square degrees of sky, photometric parameters for 10 million objects and spectra for 55,000 objects. The main access point to the data is through the website <http://archive.stsci.edu/sdss/>. The first paper to use this data [6] was submitted to astro-ph just 16 days after the release date!

The distribution of equatorial galaxies in the EDR is shown in RA-redshift wedge plots in Figure 1. The main galaxy sample is flux-limited ($r^* < 17.6$) and has a median redshift $\bar{z} \approx 0.11$. The luminous red galaxy (LRG) sample is designed to be volume-limited in the redshift range $0.2 < z < 0.38$, and also includes galaxies to $z \leq 0.5$.

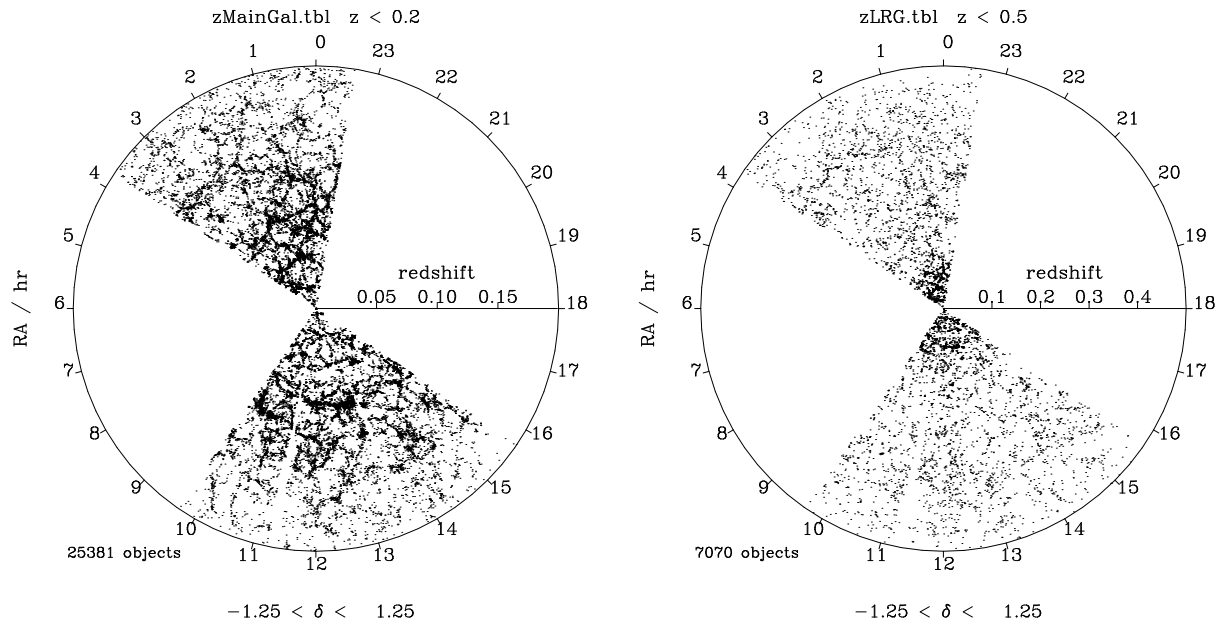


Figure 1: Distribution of EDR galaxies in RA and redshift around the equator ($|\delta| < 1.25^\circ$). The left plot shows 25,381 galaxies from the main flux-limited galaxy sample within a redshift $z = 0.2$. The right plot shows 7070 galaxies from the luminous red galaxy sample [3] to $z = 0.5$.

4 Early Science Results

I highlight some early science results which provide important constraints on the epoch of structure formation, the clustering of luminous matter and the distribution of dark matter around galaxies.

4.1 High-redshift QSOs

The SDSS has broken the $z = 6$ redshift barrier, with the discovery of a quasar at a redshift $z = 6.28$, along with two new quasars at redshifts $z = 5.82$ and $z = 5.99$ [4]. These objects were selected as *i*-dropouts: $i^* - z^* > 2.2$ and $z^* < 20.2$ ¹. Contaminating L and T dwarfs were eliminated with followup near-IR photometry and confirming spectra were obtained with the ARC 3.5m telescope. The SDSS has now observed a well-defined sample of four luminous quasars at redshift $z > 5.8$. The Eddington luminosities of these quasars are consistent with a central black hole of mass several times $10^9 M_\odot$, and with host dark matter halos of mass $\sim 10^{13} M_\odot$. The existence of such mass concentrations at redshifts $z \approx 6$, when the Universe was less than 1Gyr old, provides important constraints on models of formation of massive black holes. We expect to discover ~ 27 $z > 5.8$ quasars and one $z \approx 6.6$ quasar by the time the survey is complete. Such observations will set strong constraints on cosmological models for galaxy and quasar formation.

4.2 Large scale structure

4.2.1 Angular clustering A series of papers [1, 2, 11, 12, 13] have studied the angular clustering of galaxies in SDSS commissioning data. These papers are based on a single survey stripe (runs 752/756 observed in March 1999) measuring 2.5×90 degrees and containing some 3 million galaxies to $r^* = 22$. Star-galaxy separation is performed using a Bayesian likelihood and approximately 30% of the area is masked out due to poor seeing [11]. The angular correlation function, $w(\theta)$, is consistent with that measured from the APM Galaxy Survey [9] when scaled to the same depth [1].

An important test of the star-galaxy separation and of the photometric calibration is to check that $w(\theta)$ measured in magnitude slices scales according to Limber's equation. Figure 2 shows that the scaling of $w(\theta)$ is well-described by Limber's equation, particularly when an $\Omega_m = 0.3$, $\Omega_\Lambda = 0.7$ cosmology is assumed. Further tests for possible sources of systematic errors in the SDSS data are

¹The final SDSS photometry will be calibrated to the system denoted $u'g'r'i'z'$. The commissioning data is not yet finally calibrated so the current magnitudes are indicated with asterisks: $u^*g^*r^*i^*z^*$.

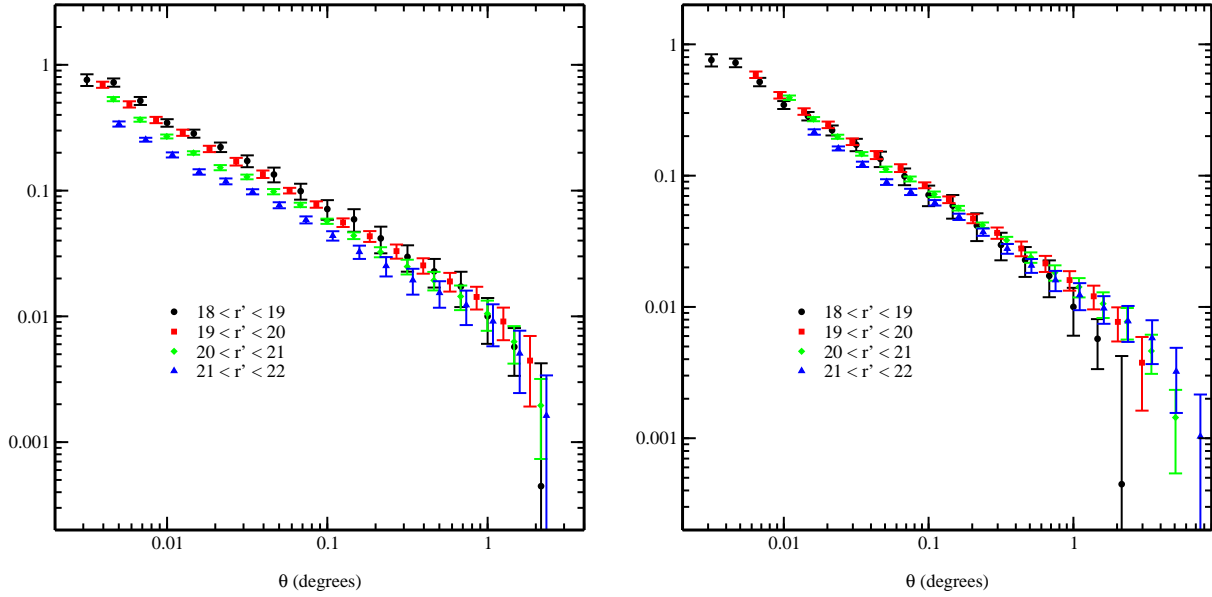


Figure 2: Scaling of the angular correlation function $w(\theta)$ measured in four magnitude slices according to Limber’s equation and assuming a selection function assumed based on the CNOC2 survey [8]. The left plot assumes a $\Omega_m = 1$, $\Omega_\Lambda = 0$ cosmology, the right plot a $\Omega_m = 0.3$, $\Omega_\Lambda = 0.7$ cosmology. Assuming the latter cosmology improves the scaling of the faintest ($21 < r' < 22$) slice. From [11].

Table 1: Power-law parameters for the real-space correlation function $\xi(r) = (r/r_0)^{-\gamma}$. Units for the correlation length r_0 are $h^{-1}\text{Mpc}$. From [15].

Sample	r_0	γ
All	6.14 ± 0.18	1.75 ± 0.03
Red	6.78 ± 0.23	1.86 ± 0.03
Blue	4.02 ± 0.25	1.41 ± 0.04
$M^* - 1.5$	7.42 ± 0.33	1.76 ± 0.04
M^*	6.28 ± 0.77	1.80 ± 0.09
$M^* + 1.5$	4.72 ± 0.44	1.86 ± 0.06

described in detail in [11] and the the angular clustering results are summarized in [1]. Other papers describe estimates of the angular power spectrum [13], inversion from $w(\theta)$ to the 3d power spectrum $P(k)$ [2] and direct estimation of power spectrum parameters [12].

4.2.2 Spatial clustering A preliminary estimate of spatial clustering of galaxies has been made using redshift information [15]. This sample consists of 29,300 galaxies with $r^* < 17.6$ and within ± 1.5 magnitudes of the characteristic magnitude M_r^* , distributed non-contiguously over 690 square degrees. The real-space correlation function $\xi(r)$ is estimated by integrating $\xi(r_p, \pi)$ over the line of sight separation π , where r_p is the projected separation of two galaxies on the sky. We find that $\xi(r)$ is well-fit over the range $0.1 < r < 30h^{-1}\text{Mpc}$ by a power law $\xi(r) = (r/r_0)^{-\gamma}$ with parameters given in Table 1. The correlation length $r_0 = 6.14h^{-1}\text{Mpc}$ is slightly larger than the $r_0 \approx 5.5h^{-1}\text{Mpc}$ found by earlier studies, presumably because dwarf galaxies with $M > M^* + 1.5$ have been excluded from this analysis. The pairwise velocity dispersion σ_{12} is consistent with 600 km/s for separations $r_p < 5h^{-1}\text{Mpc}$.

Figure 3 shows the clustering properties for two subsamples of the galaxy population selected by restframe $u - r$ colour at $(u^* - r^*)_0 = 1.8$, corresponding roughly to bulge (red) and disk (blue) dominated galaxies. The red galaxies exhibit a steeper power-law slope and longer correlation length than the blue galaxies, as indicated by the power-law fit parameters in Table 1. Also shown in Figure 3 are the correlation functions for three volume-limited samples, centered on $M^* - 1.5$, M^* and $M^* + 1.5$. The power-law slopes for these samples are all consistent with $\gamma = 1.8$, although the correlation length r_0 decreases as expected from bright to faint luminosities.

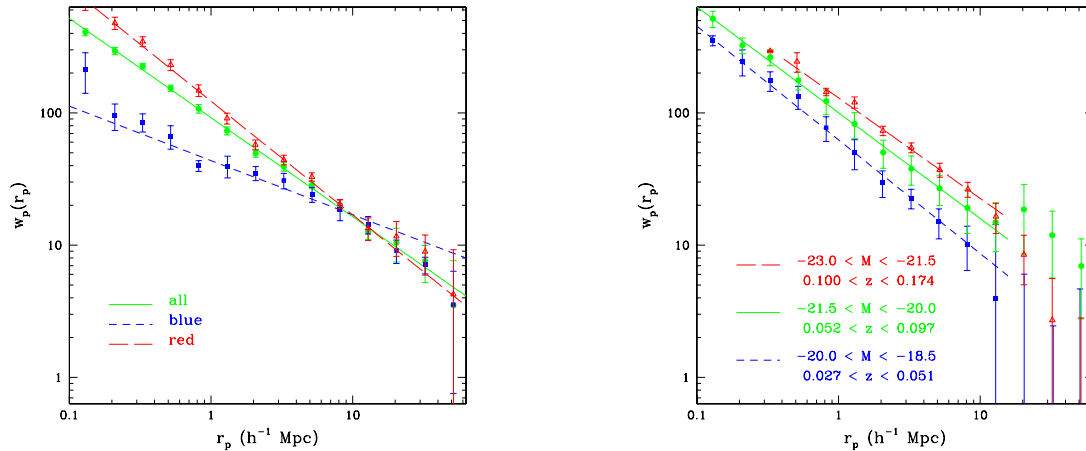


Figure 3: Projected correlation functions $w_p(r_p)$ for redshift survey galaxies subdivided by colour (left plot) and luminosity (right plot). Note that the slope of $w_p(r_p)$ increases from blue to red colour, but remains approximately constant with luminosity. From [15].

4.3 Galaxy-mass correlation function

So far, I have summarized recent SDSS results concerning the distribution of *luminous* matter in the Universe. Direct constraints on the *dark* matter distribution may be obtained from gravitational lensing. McKay et al. [10] have made weak lensing measurements of the surface mass density contrast around foreground galaxies of known redshift. Although the lensing signal is too weak to detect about any single lens, by stacking together around 31,000 lens galaxies a clear lensing signal is detected. The galaxy-mass correlation function is well fit by a power-law of the form $\Delta\Sigma_+ = 2.5(r/\text{Mpc})^{-0.8}h \text{ M}_\odot \text{ pc}^{-2}$. The strength of correlation is found to increase with the following properties of the lensing galaxy: late \rightarrow early-type morphology, luminosity in all bands apart from u' , and local density. Figure 4 shows the relationship between inferred mass within a $260h^{-1}\text{kpc}$ radius and luminosity in each of the survey bands.

5 Conclusions

The Sloan Digital Sky Survey is now fully operational and is producing high quality data at a prodigious rate. We have imaged 3135 deg^2 of sky in five colours and have obtained more than 200,000 spectra. Much exciting science has already come out of just a small fraction of the final dataset and we look forward to many more exciting discoveries in the coming years.

Acknowledgements. The Sloan Digital Sky Survey (SDSS) is a joint project of The University of Chicago, Fermilab, the Institute for Advanced Study, the Japan Participation Group, The Johns Hopkins University, the Max-Planck-Institute for Astronomy (MPIA), the Max-Planck-Institute for Astrophysics (MPA), New Mexico State University, Princeton University, the United States Naval Observatory, and the University of Washington. Apache Point Observatory, site of the SDSS telescopes, is operated by the Astrophysical Research Consortium (ARC).

Funding for the project has been provided by the Alfred P. Sloan Foundation, the SDSS member institutions, the National Aeronautics and Space Administration, the National Science Foundation, the U.S. Department of Energy, the Japanese Monbukagakusho, and the Max Planck Society. The SDSS Web site is <http://www.sdss.org/>.

Many thanks to Laurence and Marie for organizing a most enjoyable and stimulating meeting.

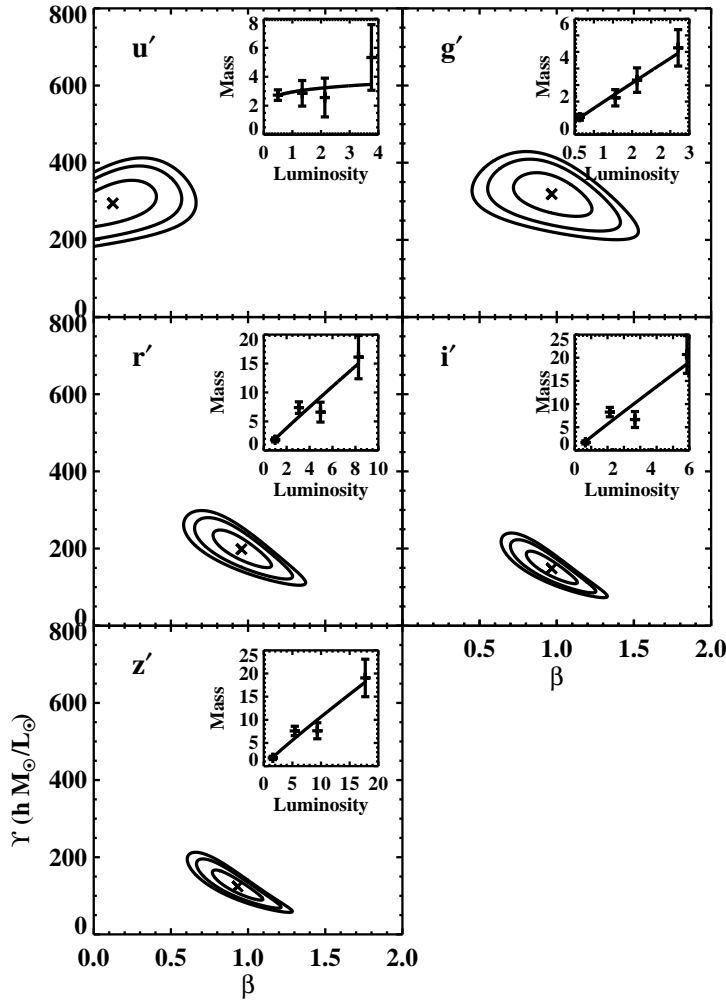


Figure 4: Mass-luminosity relation in the five SDSS bands estimated from weak lensing. The inset in each panel plots estimated mass within $260h^{-1}\text{kpc}$ (M_{260}) as a function of lens luminosity. The contours show 1, 2 and 3 sigma confidence limits on the parameters Υ and β in the relation $M_{260} = \Upsilon(L/10^{10}L_{\odot})^{\beta}$. Note that inferred mass has only very weak dependence on u -band luminosity, but in the redder survey bands *griz*, the mass-luminosity relation appears to be linear. From [10].

References

- [1] Connolly A., et al., 2001, submitted to ApJ (astro-ph/0107417)
- [2] Dodelson, S., et al., 2001, submitted to ApJ (astro-ph/0107421)
- [3] Eisenstein, D.J., et al., 2001, AJ, in press (astro-ph/0108153)
- [4] Fan, X. et al., 2001, AJ, in press (astro-ph/0108063)
- [5] Fukugita, M., et al, 1996, AJ, 111, 1748
- [6] Gaztañaga, E., 2001, submitted to MNRAS (astro-ph/0106379)
- [7] Gunn J.E., et al, 1998, AJ, 116, 3040
- [8] Lin, H., et al., 1999, ApJ, 518, 533
- [9] Maddox, S.J., Efstathiou, G., Sutherland, W.J. & Loveday, J., 1990, MNRAS, 242, 43P
- [10] McKay T.A., et al., 2001, submitted to ApJ (astro-ph/0108013)
- [11] Scranton R., et al., 2001, submitted to ApJ (astro-ph/0107416)
- [12] Szalay A.S. et al., 2001, submitted to ApJ (astro-ph/0107419)
- [13] Tegmark M., et al., 2001, submitted to ApJ (astro-ph/0107418)
- [14] York D.G., et al., 2000, AJ, 120, 1579
- [15] Zehavi I., et al., 2001, submitted to ApJ (astro-ph/0106476)